STAR Protocols

Protocol

Fabrication of gold-doped crystalline-silicon nanomembrane-based wearable temperature sensor

Step 1 — **4 hour**
Gold doping to crystalline-silicon nanomembrane (SiNM)

Step 2 — **3.5 hour**
Transfer gold-doped crystalline-SiNM to flexible substrate

Step 3 — **8.5 hour**
Define serpentine mesh structured device

Step 4 — **6 hour**
Body temperature and respiration monitoring

Kyowon Kang,
Mingyu Sang,
Baoxing Xu, Ki Jun
Yu

kijunyu@yonsei.ac.kr

Highlights

Gold-doped
crystalline silicon
nanomembrane with
ultrahigh thermal
sensitivity

Protocol is amenable
to modulating
properties of silicon
with gold doping
mechanism

Detailed fabrication
process for
serpentine mesh-
structured epidermal
electronics

Continuous body
temperature
monitoring with gold-
doped SiNM
wearable sensor

Wearable temperature sensors with high thermal sensitivity are required for precise and continuous body temperature monitoring. Here, we present a protocol for fabricating a thin, stretchable, and ultrahigh thermal-sensitive wearable sensor based on gold-doped crystalline-silicon nanomembrane (SiNM). We provide detailed steps of gold doping technique to SiNM and fabrication processes for gold-doped crystalline-SiNM-based wearable temperature sensor.

Publisher's note: Undertaking any experimental protocol requires adherence to local institutional guidelines for laboratory safety and ethics.

Protocol

Fabrication of gold-doped crystalline-silicon nanomembrane-based wearable temperature sensor

Kyowon Kang,[1,4] Mingyu Sang,[1,4] Baoxing Xu,[3] and Ki Jun Yu[1,2,5,6,*]

[1]School of Electrical and Electronic Engineering, Yonsei University, 50 Yonsei-ro, Seodaemungu, Seoul 03722, Republic of Korea

[2]School of Electrical and Electronic Engineering, YU-KIST Institute, Yonsei University, 50 Yonsei-ro, Seodaemungu, Seoul 03722, Republic of Korea

[3]Department of Mechanical and Aerospace Engineering, University of Virginia, Charlottesville, VA 22904, USA

[4]These authors contributed equally

[5]Technical contact

[6]Lead contact

*Correspondence: kijunyu@yonsei.ac.kr
https://doi.org/10.1016/j.xpro.2022.101925

SUMMARY

Wearable temperature sensors with high thermal sensitivity are required for precise and continuous body temperature monitoring. Here, we present a protocol for fabricating a thin, stretchable, and ultrahigh thermal-sensitive wearable sensor based on gold-doped crystalline-silicon nanomembrane (SiNM). We provide detailed steps of gold doping technique to SiNM and fabrication processes for gold-doped crystalline-SiNM based wearable temperature sensor.
For complete details on the use and execution of this protocol, please refer to Sang et al. (2022).[1]

BEFORE YOU BEGIN

Accurate and continuous measurement of body temperature is a useful criterion in early diagnosis and treatment of various diseases such as Coronavirus-19 (COVID-19), pulmonological diseases, cardiovascular related diseases and wound healing.[2] Therefore, temperature measurement technology that can continuously measure body temperature with high thermal sensitivity and accuracy is essential.[3–5] A lightweight wearable temperature sensor is an emerging measurement method that can measure the temperature change precisely and minimize discomfort when attached on skin. Moreover, it can monitor temperature changes continuously in a real-time manner, even when the skin is subjected to mechanical deformation in accommodation with human body motions.[6]

Silicon, a widely used representative inorganic material with high reliability, has oxidation resistance property and fast response time for the active electronic material, while conventional organic materials are vulnerable to oxidation and have slow response times.[7–10] Meanwhile, a doping process that injects impurities can modulate the properties of silicon, such as temperature coefficient of resistance (TCR), piezo-resistance and electrical conductance. III-V atoms (boron, arsenic, phosphorous, etc.) are widely used fast diffusing impurities for silicon doping, while gold is a typical slow diffusing (deep impurity) material. When a gold atom, which has amphoteric property, diffuses into silicon via the Kick-out and Frank-Trunbull mechanisms, the ionized gold atom recombines with an electron (or hole) of n-type (or p-type) silicon. Diffused gold atoms compensate for donors (or acceptors), resulting in an increment in resistivity of silicon. The maximum resistance can be achieved when gold atom concentration compensates for donor (or acceptor) concentration. Because of the modulation of the

fermi energy level by gold doping of Si, the intrinsic energy level of Si shifts from the intrinsic region to the freeze-out region, where the extrinsic region is minimized in the temperature-resistance plot.[1] This can dramatically increase the thermal sensitivity of Si in the low temperature sensing region. When heat is applied to the gold doped silicon, electron density increases and mobility decreases, where electron density plays a dominant role in resistivity with temperature change. Simultaneously, electron-hole pairs are formed, the number of free electrons increases, and the resistance decreases, resulting in a negative TCR property.[11–23]

Here, we present an experimental protocol for fabricating an ultrathin, stretchable, and highly thermal sensitive wearable temperature sensor by doping SiNM with gold atoms. Doping gold atoms to silicon shifts the fermi energy level, which induces a change in the activation energy level and results in high thermal sensitivity. Gold-doped SiNM has TCR of -37270.72 ppm $°C^{-1}$, which makes it 22 times more sensitive than that of conventional metal-based thermal sensor. In addition, the gold-doped SiNM based temperature sensor has a rapid response time ($\sim$8 ms), which indicates the capability of real-time monitoring with a highly sensitive inorganic material-based temperature sensor. The thickness of the gold-doped SiNM based wearable temperature sensor is only 3.4 μm, which is thin enough to be attached to the skin via Van der Waals force. In addition, by placing the temperature sensing gold-doped SiNM on the neutral mechanical plane (NMP) and island-to-island structure with interconnections of a serpentine mesh structure, the reliability of temperature sensing performance and stretchability has been accomplished. Our protocol can be highlighted by demonstrating step-by-step detailed fabrication process for wearable temperature sensor based on gold-doped SiNM, which paves the way for the wide applicability and scalability of silicon by modulating the property of silicon with a novel gold doping process.

Preparation of SOI wafer

⏱ Timing: 1 h

1. Prepare an 8-inch silicon-on-insulator (SOI) wafer with 100 orientations. Cut the SOI wafer into a proper size with wafer cutter.
2. Prepare a 95% sulfuric acid solution and 30% hydrogen peroxide solution for piranha solution. Measure 100 mL of sulfuric acid and heat it on a hot plate set to 100°C for 5 min.

   △ CRITICAL: Sulfuric acid used for piranha solution which is hazardous should be stored in acid cabinet for safety. Extra caution is needed when preparing the piranha solution and the entire process must be done in fume hood for ventilation since the piranha solution is corrosive and extremely dangerous. Researchers should follow the designated disposal process of piranha solution.

3. Mix 25 mL of hydrogen peroxide solution to the heated sulfuric acid. Wait until vigorous chemical reaction between sulfuric acid and hydrogen peroxide to finish.
4. Soak the prepared SOI wafer into the piranha solution for 20 min.
5. Prepare the de-ionized (DI) water and soak a piranha solution cleaned SOI wafer in it.
6. Change the DI water three times to rinse off the residual piranha solution.

Preparation of equipment

⏱ Timing: 4 h

7. Change the quartz tube of the tube furnace to a gold doping quartz tube (Figure 1A).
8. Turn on the tube furnace and set the oxygen flow rate to 20 SCCM.
9. Set the temperature of the tube furnace between 1,000°C - 1,100°C.
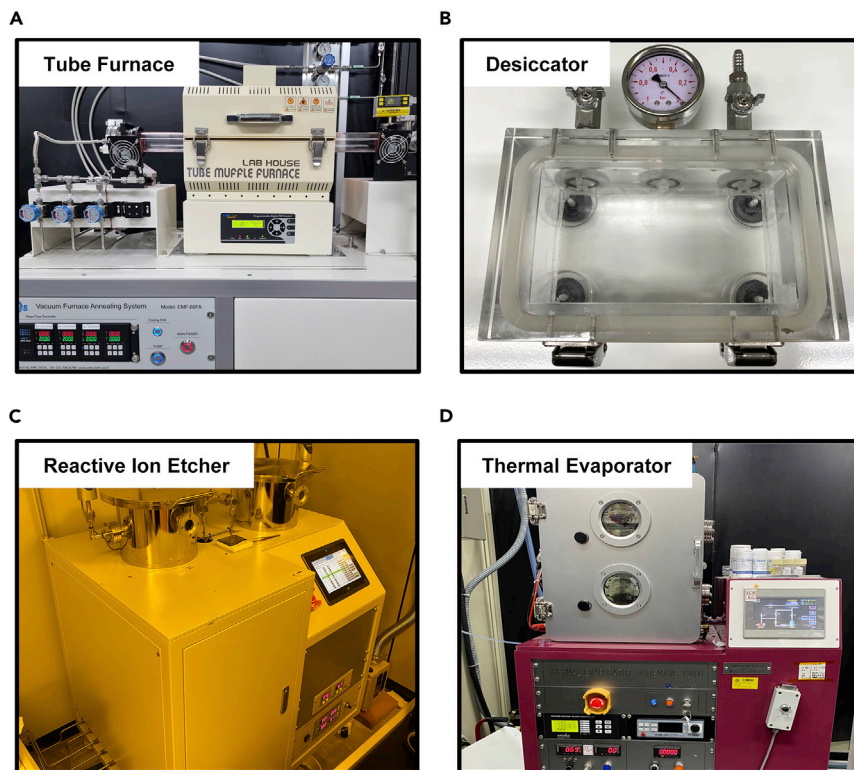
Figure 1. Equipment for fabricating ultra-high thermal sensitive wearable sensor based on gold-doped crystalline-SiNM
(A) Furnace.
(B) Desiccator.
(C) Reactive ion etcher (RIE).
(D) Thermal evaporator.

10. After the tube furnace reaches the set temperature, close the rotary valve (R/V) and change the oxygen flow rate to 200 SCCM for ventilation.

> ⚠ CRITICAL: The designated quartz tube for gold doping is essential to prohibit cross contamination.

Preparation of polydimethylsiloxane (PDMS) stamp

🕓 Timing: 50 h

11. Prepare a PDMS solution. Measure 40 g of base and 10 g of curing agent for PDMS; mix them.
12. Place the mixed PDMS solution on a desiccator and vacuum for 1 h. The desiccator is shown in Figure 1B.
13. Slowly pour the vacuumed PDMS solution into a square petri dish (125 mm × 125 mm) until the height reaches 12 mm.
14. Store the PDMS solution at room temperature for 48 h in a fume hood.
15. Prepare a slide glass substrate. Clean the slide glass with acetone, rinse with isopropanol (IPA) and DI water. To increase adhesion of the slide glass surface, O_2 plasma treatment is performed using reactive ion etching (RIE) (Figure 1C).
16. Cut the fully cured PDMS into cuboid shapes with a razor blade and attach the PDMS to the slide glass substrate.

KEY RESOURCES TABLE

REAGENT or RESOURCE	SOURCE	IDENTIFIER
Chemicals, peptides, and recombinant proteins		
Acetone	DUKSAN	CAS: 67-64-4
Isopropanol (IPA)	DUKSAN	CAS: 67-63-0
De-ionized (DI) water	N/A	N/A
Sulfuric acid (H_2SO_4)	DUKSAN	CAS: 7664-93-9
Hydrogen peroxide	SAMCHUN	7722-84-1
Hydrofluoric acid (HF)	DUKSAN	CAS: 7664-39-3
6:1 Buffered oxide etch (6:1 BOE)	DUKSAN	CAS: 7664-93-9
Silicon-on-insulator (SOI)	Soitec	https://www.soitec.com/en/products/connect-fd-soi
Polydimethylsiloxane (PDMS)	DOW	https://www.dow.com/en-us/pdp.sylgard-184-silicone-elastomer-kit.01064291z.html#overview
Poly(pyromellitic dianhydride-co-4,4′-oxydianiline), amic acid solution (polyimide solution)	ALDRICH	https://www.sigmaaldrich.com/product/aldrich/575798
Ethylene glycol	DUKSAN	CAS: 107-21-1
Gold (Au)	TAEWON SCIENTIFIC CO.	CAS: 7440-57-5
Copper (Cu)	TAEWON SCIENTIFIC CO.	CAS: 7440-50-8
Chrome (Cr)	TAEWON SCIENTIFIC CO.	CAS: 7440-47-3
S1805 photoresist	DOW	MICROPOSIT™ S1805™ G2 POSITIVE PHOTORESIST
AZ 5214 photoresist	AZ Electronic Materials	https://www.microchemicals.com/products/photoresists/az_5214_e.html
AZ nLOF 2035 photoresist	AZ Electronic Materials	https://www.microchemicals.com/products/photoresists/az_nlof_2035.html
AZ 300 MIF developer	AZ Electronic Materials	https://www.microchemicals.com/products/developers/mif_developers.html
Anisotropic conductive film cable (ACF cable)	Elform	P/N HST-9805-210
Water-soluble tape	3M Electronic Specialty	https://www.3m.com/3M/en_US/p/d/b00042264/
Other		
Wafer cutter	AS-ONE	6-539-05
Hot plate	Daihan Science	DH-WMH02503-EA
Tube furnace	E.M.S Tech	N/A
Desiccator	Daihan Science	DH.DeVS
Fume hood	C&C Lab	H-GE.1280
Razor blade	DORCO	DN52
Slide glass	SUPERIOR	HSU-1000412
Thermal evaporator	KOREA VACUUM TECH	KVE-T2000
Spin coater	DONG AH TRADE CORP.	Spin Coater ACE-200
UV aligner	MIDAS SYSTEM	MDA-400S
Reactive ion etcher (RIE)	YOUNG HIGH TECH	N/A
UV ozone cleaner	UV SMT	http://www.uvsmt.com/sub/sub_uvo3_02.php
Vacuum oven	SH SCIENTIFIC	SH-VDO-08NG
Digital multimeter	KEITHELY	DAQ 6510
Data acquisition system (DAQ)	NATIONAL INSTRUMENTS CORP	PXIe-8840, PXIe-6365, PXIe-6738
Infrared (IR) camera	PeakTech	PeakTech 4980

STEP-BY-STEP METHOD DETAILS

Gold doping of SOI wafer

⊙ Timing: 4 h

In this work, to modulate the property of silicon, a thin layer of gold was deposited on the piranha cleaned SOI wafer using a thermal evaporator and annealing was performed at 1,000°C–1,100°C to
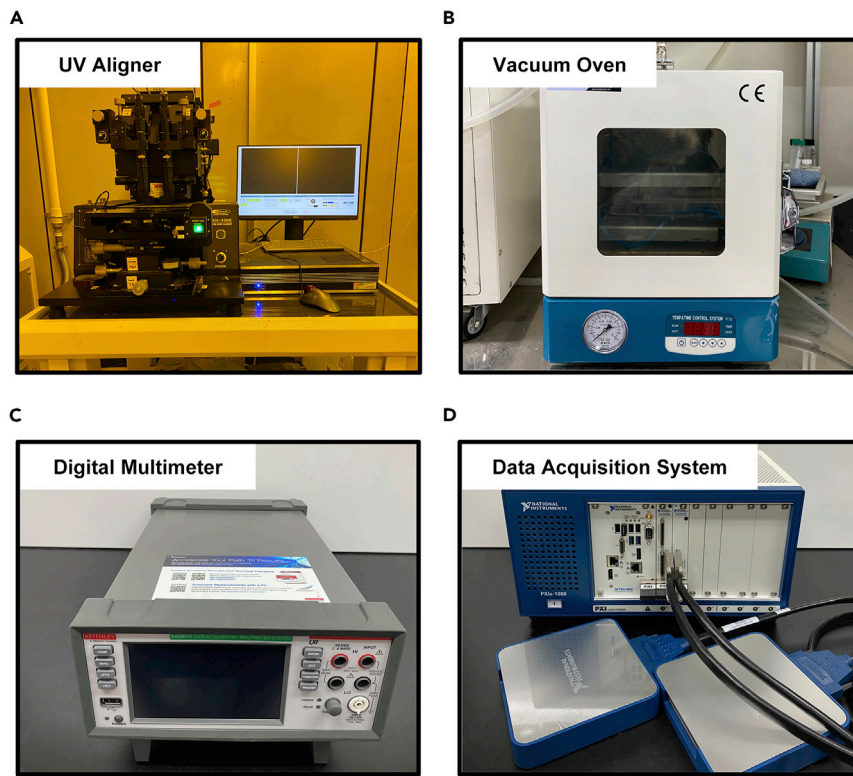
Figure 2. Equipment for fabricating ultra-high thermal sensitive wearable sensor based on gold-doped crystalline-SiNM
(A) Aligner.
(B) Vacuum oven.
(C) Digital multimeter.
(D) Data acquisition system (DAQ).

diffuse the gold atoms in the SiNM of the SOI wafer (Figure 3). Above an annealing temperature of 1,000°C, gold atoms quickly diffuse into silicon via the Frank-Turnbull and Kick-out mechanisms. The diffused gold atoms induce a movement of the fermi energy level to intrinsic level and shift freeze-out region of silicon to intrinsic region which results in ultra-high thermal sensitivity at a low temperature sensing range (25°C–45°C) (Figure 4).

1. Dip the piranha cleaned SOI wafer in the 6:1 BOE for 2 s to remove native oxide and chemical oxide.
2. Rinse the BOE with DI water.

> △ CRITICAL: The surface of SOI wafer is hydrophobic after BOE treatment due to the removal of native oxide and chemical oxide. Researchers must be careful when using BOE since it is a very hazardous chemical.

3. Immediately attach the SOI wafer to a stage of thermal evaporator and deposit the thin layer of gold (10 nm) (Figure 1D).
   a. Turn on the Roughing valve (R/V) of the thermal evaporator and wait until the vacuum level of 5×10^{-2} Torr is reached.
   b. Turn off the R/V and turn on the Foreline valve (F/V) and Main valve (M/V) for achieving low pressure vacuum. Turn on the ion gauge to check the vacuum level of the chamber.
   c. After vacuum level reaches 5×10^{-6} Torr, start evaporating the gold.
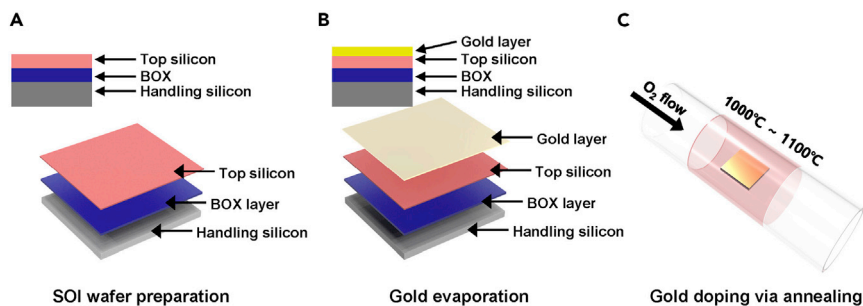
Figure 3. Gold doping process
(A) Prepare SOI wafer by piranha cleaning and remove chemical oxide with BOE.
(B) Deposit the gold layer using thermal evaporator.
(C) Annealing the gold deposited SOI wafer in the furnace with O_2 ambient condition for diffusing gold atoms into SiNM. Figure reprinted with permission from Sang et al.[1]

4. Place the SOI wafer with the thin layer of gold in a pre-heated tube furnace (above 1,000°C) for 2 h in ambient oxygen environment. troubleshooting section (problem 1).
5. After 2 h of annealing, put the gold-doped SOI wafer in ethylene glycol solution to prohibit out-diffusion of gold atoms during cooling down to Room temperature (RT, 25°C). troubleshooting section (problem 2).
6. Put the gold-doped SOI wafer to 49% HF solution for 30 s–60 s to remove the oxide formed during annealing.
7. Rinse with DI water to remove residual HF solution.

Transfer gold-doped crystalline-silicon nanomembrane

⊙ Timing: 3.5 h

Conventional crystalline-silicon has a high Young's modulus in the gigapascal range (92 GPa–202 GPa), which is generally brittle when a bending force is applied. Unlike the conventional silicon wafer with a thickness of a few hundred micrometers, when the thickness of crystalline-silicon is reduced to the nanometer scale (<300 nm), flexural rigidity is reduced to more than nine orders of magnitude, resulting in flexible properties.[24–28] Because handling the nanometer-scale membrane by itself is difficult, transferring it to a flexible substrate is essential for the post-fabrication process. Therefore, transferring the silicon nanomembrane (thickness of 300 nm) to an ultra-thin layer of a flexible substrate after gold doping is critically important process for flexibility (Figures 5A–5C). This flexibility and ultra-thin thickness enable conformal contact between the human skin and the device which allows precise temperature monitoring.

8. Spin-coat S1805 photoresist on gold-doped SOI wafer at 3,000 rpm for 60 s.
9. Bake at 110°C for 60 s on a hotplate.
10. Pattern the hole pattern (hole diameter: 3 μm, pitch: 50 μm) on soft-baked photoresist using UV aligner (Figure 2A) with an exposure time of 7 s.
11. Develop the hole pattern with the AZ 300 MIF developer for 60 s.
12. Dry-etch the patterned top silicon of the gold-doped SOI wafer with RIE (SF_6, 20 SCCM, 150 W, 50 s).
13. Sink the dry-etched SOI wafer in 49% HF solution until the box layer of the SOI wafer is fully dissolved. When the box layer of the SOI wafer is fully dissolved by the HF solution, the color of the top silicon will be darker.
14. Pick up the SOI wafer from the HF solution and move it to a DI water bath to rinse the residual HF solution.
15. Carefully blow off the DI water with pure N_2 gas.
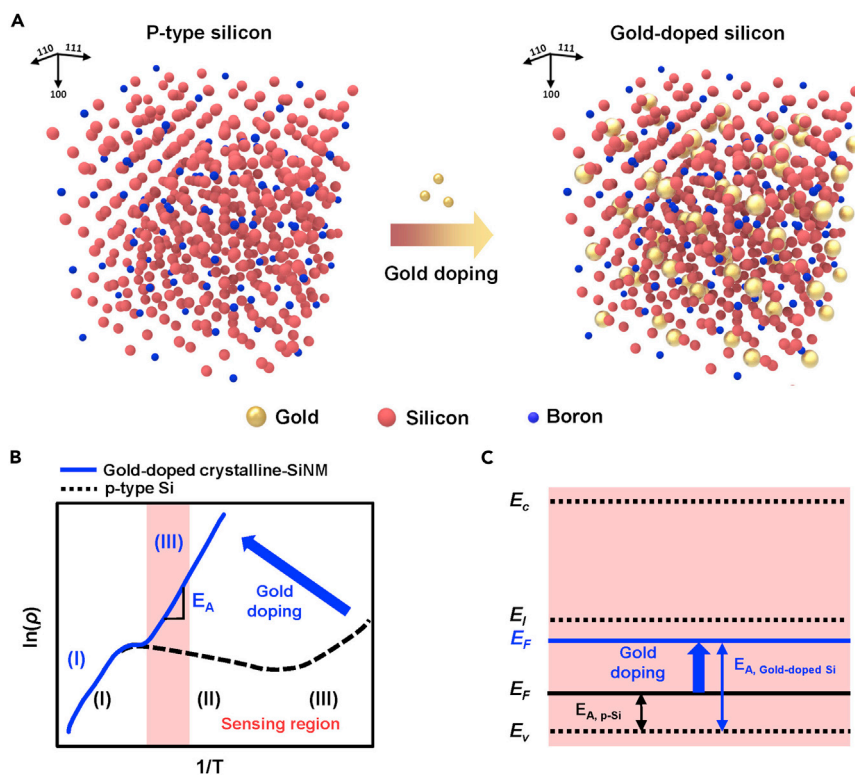
Figure 4. Silicon property modification after gold doping of SiNM

(A) Schematic figure of before and after gold doping of silicon.

(B) Shift of resistivity-temperature curve after gold doping process (I: intrinsic region, II: extrinsic region, III: freeze-out region).

(C) Energy band diagram of silicon after gold doping process. Figure reprinted with permission from Sang et al.[1]

16. To transfer the gold-doped SiNM of the SOI wafer to the PDMS stamp, apply the PDMS stamp on the dehydrated SOI wafer by contacting the edge of the tilted stamp to SOI wafer.

17. Slowly lower the opposite side of the PDMS stamp that contacts the edge of the SOI wafer so that the entire SOI wafer is sticked to PDMS stamp.

⚠ CRITICAL: When applying the PDMS stamp to dehydrated SOI wafer, make sure no air bubbles are trapped between the SOI wafer and the PDMS stamp.

18. The gold-doped SiNM is detached from the SOI wafer by applying instantaneous force with finger to the edge of the glass substrate with PDMS stamp.

19. Prepare the glass substrate cleaned with acetone, IPA and DI water.

20. Spin-coat the degassed PDMS at 3,000 rpm and cure at 70°C for 1 h and 110°C for 2 h.

21. 20 min of UV treatment on the surface of cured PDMS is required before spin-coating the poly(-pyromellitic dianhydride-co-4,4′-oxydianiline), amic acid solution (polyimide solution).

22. Spin-coat the polyimide solution at 3,000 rpm on pre-treated PDMS.

23. Bake at 110°C for 30–40 s.

24. Slightly attaching the PDMS stamp with the transferred gold-doped SINM (step 18) to the soft-baked polyimide (step 23) with the same method described in step 16 and step 17.

25. Bake at 110°C for 60 s and peel off the PDMS stamp.

26. Bake at 150°C for 5 min.

27. Remove the hole-patterned photoresist with acetone, IPA and DI water.

28. Hard-bake the transferred sample in a vacuum oven (Figure 2B) with 210°C for 2 h.
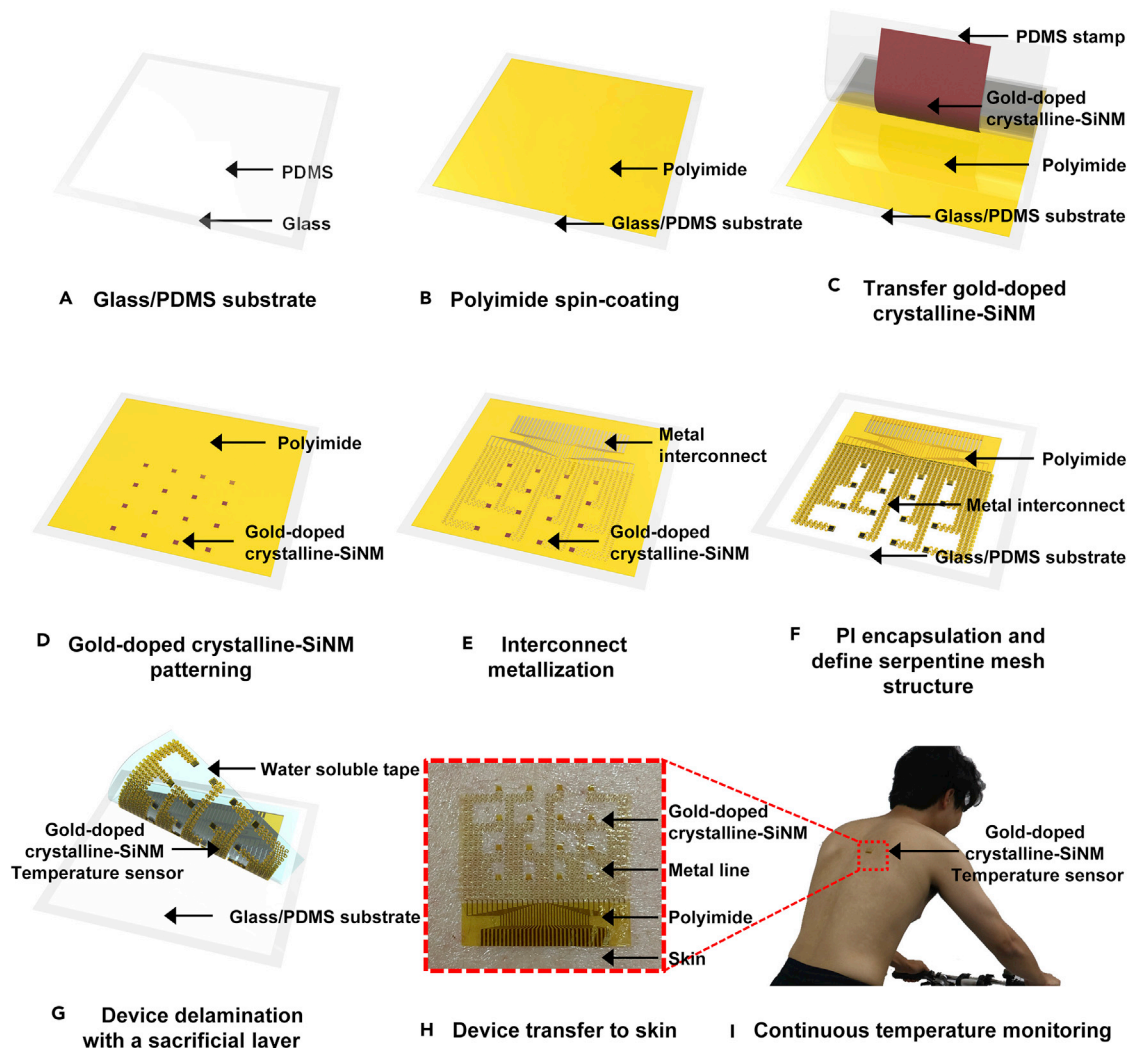
Figure 5. Fabrication process of gold-doped crystalline-SiNM temperature sensor array with ultra-high thermal sensitivity
(A) Preparing glass/PDMS substrate.
(B) Preparing substrate by spin-coating PI layer on PDMS.
(C) Transferring gold-doped crystalline-SiNM on PI with PDMS stamp.
(D) Pattering and etching gold-doped crystalline-SiNM.
(E) Metallization.
(F) PI encapsulation and defining the entire device into mesh structure.
(G) Delaminating the device with water-soluble tape.
(H) Transferring the device onto the target skin.
(I) Continuous and precise monitoring of body temperature precisely. Figure reprinted with permission from Sang et al.[1]

Defining serpentine mesh structured device

© Timing: 8.5 h

The ultra-thin device with a total thickness of under 3.5 μm can be conformally attached to the skin through the Van der Waals force. In addition, the serpentine mesh interconnect with an island structure allows stretchability by minimizing the strain effect on temperature sensing area while a stretching force is applied (Figures 5D–5F). This novel structure secures the reliability of the device under multidirectional deformations such as expansion, contraction and bending (Figure 6). It also allows
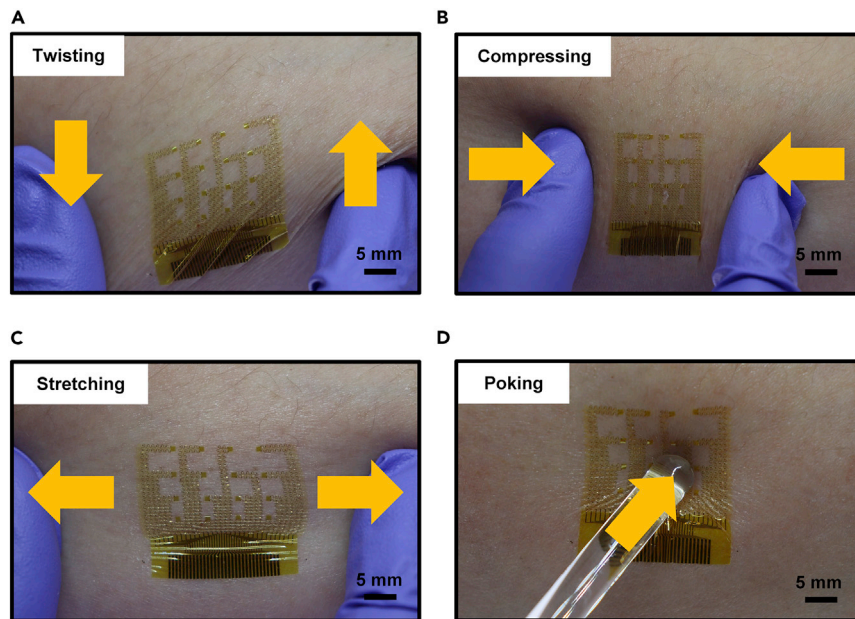
Figure 6. Gold-doped crystalline-silicon nanomembrane temperature sensor array on the skin with physical deformation is applied
(A) Twisting.
(B) Compressing.
(C) Stretching.
(D) Poking. Figure reprinted with permission from Sang et al.[1]

skin waste such as sweat and sebum to be drained and maintains adhesion so that the device adheres well to the skin with good ventilation.

29. Spin-coat AZ nLOF 2035 at 3,000 rpm for 30 s and bake for 60 s on a 110°C hot plate.
30. Expose it to UV light using a patterned mask.
31. Post-bake for 60 s on a 110°C hot plate. Develop photoresist with AZ 300 MIF developer for 40 s and rinse with DI water.
32. Remove native oxide of gold-doped SiNM by dipping into 6:1 BOE for 30 s and rinse with DI water.
33. Deposit 5 nm of chrome and 200 nm of gold via thermal evaporation.
34. Lift off the sacrificial metal layer by immersing it in acetone at 40°C. Rinse with IPA and DI water.
35. Spin-coat an additional PI layer for an encapsulation layer. After spin-coating PI at 3,000 rpm for 30 s, cure at 110°C for 30 min, 150°C for 30 min, 180°C for 30 min, and at 210°C for 2 h.

> △ CRITICAL: When curing the polyimide after spin coating, ramp up the annealing temperature step-by-step to minimize the shrinking due to the sudden increment in temperature.

36. Deposit 200 nm of copper using thermal evaporation as a hard mask for PI etching.
37. Using AZ 5214 photoresist, pattern the copper. Spin-coat AZ 5214 at 3,000 rpm for 30 s and bake for 110 s on a 110°C hot plate.
38. Expose it to UV light using a serpentine mesh shaped mask on which the PI will be patterned. Develop using AZ 300 MIF for 90 s and rinse with DI water.
39. Etch copper with copper etchant, clean with DI water, and blow thoroughly with N_2 gas.
40. Remove photoresist with acetone and rinse with IPA and DI water.
41. Etch PI with O_2 plasma using RIE (O_2, 100 SCCM, 200 W, 20 min).
42. Remove the remaining copper with copper etchant and clean with DI water.
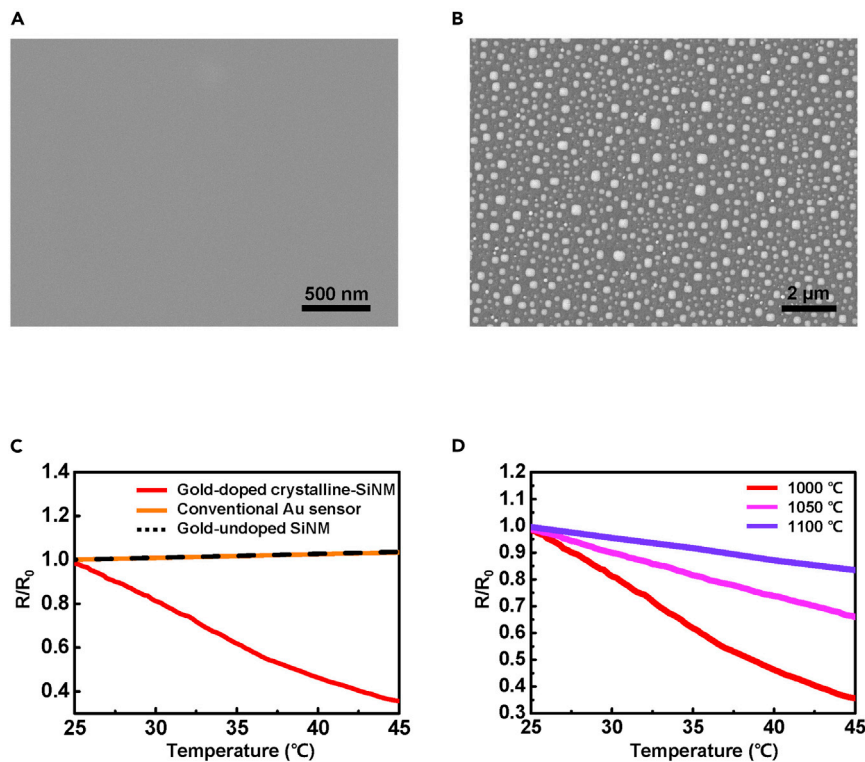
Figure 7. Thermal property validation of the gold-doped crystalline-silicon nanomembrane
(A) SEM image of crystalline-SiNM.
(B) SEM image of gold-doped crystalline-SiNM.
(C) Relative resistance response to temperature of gold-doped crystalline-SiNM (red line), metal (orange line) and gold-undoped SiNM (dashed line) temperature sensor.
(D) Relative resistance response to temperature of gold-doped crystalline-SiNM temperature sensor under different annealing temperatures; 1,000°C (red line), 1,050°C (pink line) and 1,100°C (purple line). Figure reprinted with permission from Sang et al.[1]

Body temperature and respiration monitoring

© Timing: 6 h

Since gold-doped SiNM is sandwiched between PI, strain applied to the gold-doped SiNM can be minimized while external tensile or compressive strain is applied. Even in situations of intense exercise such as cycling, the gold-doped SiNM based temperature sensor array can monitor body temperature continuously without being affected by sweat or movement and can also precisely monitor small temperature changes that occur during respiration.

43. Connect the gold-doped SiNM based temperature sensor array to the measuring equipment; i.e., DAQ, using an ACF cable (Figures 2C and 2D). The ACF cable is attached using a soldering iron at 130°C.
44. Attach water-soluble tape to the device and slowly peel off the device from the glass/PDMS substrate (Figure 5G).

⚠ CRITICAL: Because water-soluble tape is susceptible to moisture, storing it under a vacuum state and placing in a desiccator before use is recommended.

45. Attach the device with the water-soluble tape to the skin of the area to be measured.

46. Dissolve the water-soluble tape completely with DI water.
47. We used a conventional metal-based temperature sensor as a control, attached it beside to the gold-doped SiNM temperature sensor and proceeded simultaneous measurement for both sensors.
48. The position for continuous body temperature measurement during exercise is the central part of the back, and the position for monitoring temperature change during respiration is the philtrum. The temperature change during inhalation and exhalation was measured using an IR camera, and the experiment was conducted on this basis (Figures 5H and 5I).

EXPECTED OUTCOMES

Silicon has high reliability under various working conditions, can be processed at high temperatures, has high biocompatibility, and is widely used for fabricating electronic devices such as transistors because of its oxidation resistance compared to organic materials.[29] In addition, the fast thermal response speed of silicon-based sensors is a great advantage. This protocol identifies that the band gap of semiconductors can be controlled through the fusion of semiconductors and metals at high temperatures, and utilizes this to develop into ultra-sensitive, flexible thermal sensors. We have successfully doped gold into silicon nanomembrane using novel strategy (Figures 7A and 7B). Accordingly, we developed a wearable temperature sensor array with high precision and ultra-high sensitivity with a TCR of -37270.72 ppm $^\circ C^{-1}$, one of the highest levels of thermal sensitivity. Gold-doped SiNM temperature sensor has 22 times higher thermal sensitivity compared to conventional metal-based temperature sensor (Figures 7C and 7D).

Precisely and continuously measuring the temperature attaching the device to the skin conformally without being affected by movement or the external environment is very important. This protocol implements an ultra-thin device with a total thickness of less than 3.5 μm by applying a sandwich structure using PI, so that the gold-doped SiNM located in NMP can minimize the effect of deformation. In addition, it was designed in the form of a serpentine mesh with an island-to-island structure to maintain performance under a multidirectional deformation of 30% and to be advantageous for sweat drainage and ventilation (Figure 8A). Even with the encapsulation layer, the gold-doped SiNM temperature sensor array shows a rapid response time (detailed experiments and results are included in the Sang et al.[1]).

We confirmed that our wearable temperature sensor array with gold-doped SiNM can monitor the temperature change precisely with low hysteresis and high reliability (Figures 8B–8E). Precise and continuous body temperature measurement and breathing monitoring are possible during extreme exercise such as cycling. This paves the way for human health management, precise diagnosis, and research on the relationship between body temperature and disease (for details see Sang et al.[1]). In addition, the energy level modulation and property change of silicon through gold doping has infinite potential for future development of various sensors and electrical as well as electronic applications.

LIMITATIONS

A limitation exists in the transfer process of gold-doped SiNM using PDMS stamps performed in a laboratory environment. The size of gold-doped SiNM that can be transferred is determined according to the PDMS stamp size. The transfer of a large area size over a certain level has a limitation in that the yield is reduced. To fabricate 4 × 4 arrays of gold-doped SiNM based temperature sensor, we transferred without any problems up to 2.5 × 2.5 cm size according to the above mentioned conditions. However, for a larger size, establishing optimal conditions for the transfer process is necessary, such as adjusting the size of the stamp according to the size of the device to be manufactured and controlling the curing time. In addition, for the etching-induced floating of film structures on the liquid solutions that is considered an etching failure and cannot be transferred by the intermediate
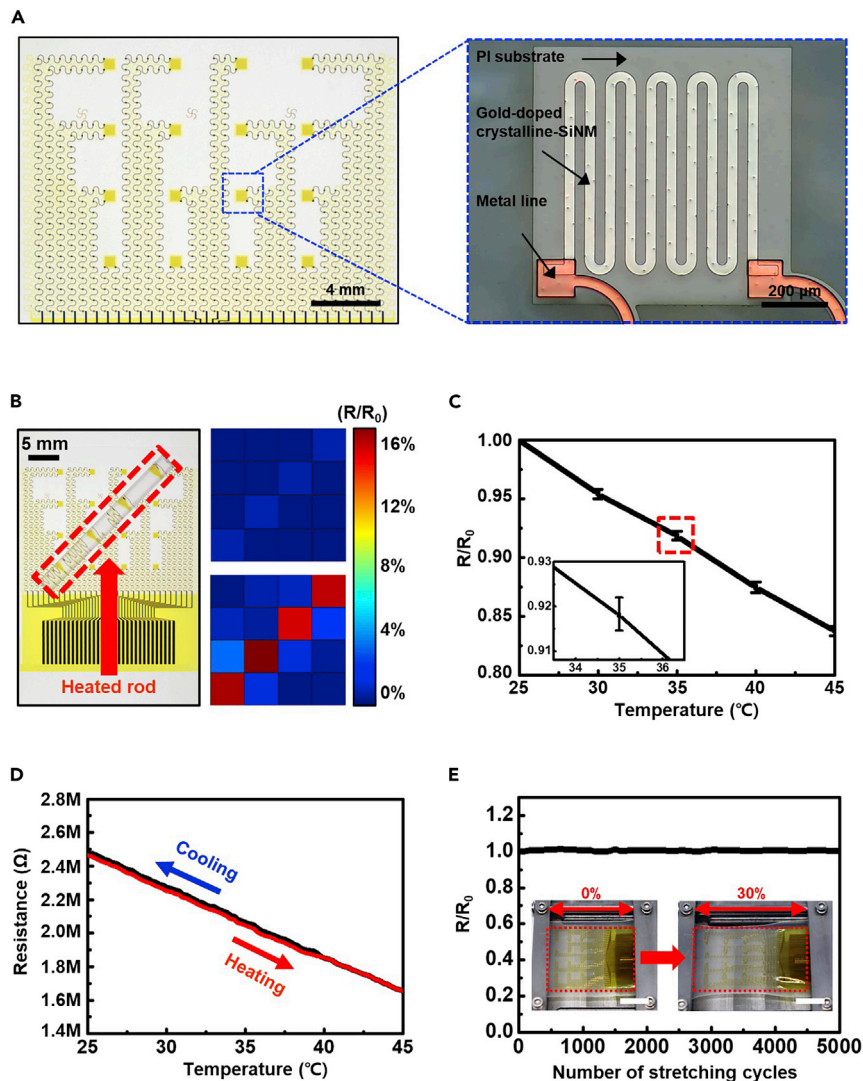
Figure 8. Optical images and evaluation results of thermal and mechanical properties of the gold-doped crystalline-SiNM based temperature sensor array

(A) Image of the gold-doped crystalline-SiNM temperature sensor array (left) and magnified image of the single temperature sensing cell.

(B) Image (left) and temperature monitoring heat map result (right) of the conventional metal temperature sensor array (top) and the gold-doped crystalline-SiNM based temperature sensor array (bottom) using heated rod.

(C) Cell-to-cell variation graph of and the gold-doped crystalline-SiNM based temperature sensor array and magnified graph of error bar (inset).

(D) Hysteresis result of cooling down (blue) and heating up (red) the gold-doped crystalline-SiNM based temperature sensor array.

(E) 30% uniaxial stretching cycle test of the gold-doped crystalline-SiNM based temperature sensor array.

Figure reprinted with permission from Sang et al.[1]

soft PDMS stamp, capillary transfer that enables the direct transfer from liquid[30,31] could be explored in the future.

TROUBLESHOOTING

Problem 1

The deposited thin gold nanofilm stacked on a silicon wafer can be evaporated without diffusion during high-temperature processing in a furnace. For example, if a 10 nm gold-stacked silicon wafer is

placed in a furnace at RT and the temperature is raised to 1,000°C or higher, the gold melts and is blown away before the target temperature is reached; therefore, the diffusion process is not completed properly.

Potential solution

After raising the temperature inside the furnace to the target doping temperature, insert the sample. For example, if silicon with 10 nm of gold is placed in a furnace maintained at 1,000°C, gold rapidly diffuses into the silicon before the gold melting and being blown away.

Problem 2

After the doping is finished, when gold-doped SiNM is taken out from the high-temperature furnace and cooled down at RT, out-diffusion occurs which cause poor reliability of gold doping concentration.

Potential solution

Ethylene glycol which has a high thermal conductivity ($0.254\ Wm^{-1}\ K^{-1}$) is a possible solution to prohibit out-diffusion of gold atoms. Cooling down the gold-doped SiNM in ethylene glycol solution after the doping process with high an annealing temperature can minimize the out-diffusion of gold atoms.

RESOURCE AVAILABILITY

Lead contact

Further information and requests for resources and reagents should be directed to and will be fulfilled by the lead contact, Ki Jun Yu (kijunyu@yonsei.ac.kr).

Materials availability

This study did not generate new unique reagents.

Data and code availability

All data reported in this paper will be shared by the lead contact upon request.

No code was generated in this study.

AUTHOR CONTRIBUTIONS

K.K. and M.S. contributed equally to this work. K.J.Y., B.X., K.K., and M.S. conceived the idea. K.K. and M.S. performed the experiments and wrote the manuscript. K.J.Y. supervised the entire study. All authors commented on the manuscript.

DECLARATION OF INTERESTS

The authors declare no competing interests.

REFERENCES

1. Sang, M., Kang, K., Zhang, Y., Zhang, H., Kim, K., Cho, M., Shin, J., Hong, J.-H., Kim, T., Lee, S.K., et al. (2022). Ultrahigh sensitive Au-doped silicon nanomembrane based wearable sensor arrays for continuous skin temperature monitoring with high precision. Adv. Mater. *34*, 2105865. https://doi.org/10.1002/adma.202105865.

2. Kim, D.-H., Lu, N., Ma, R., Kim, Y.-S., Kim, R.-H., Wang, S., Wu, J., Won, S.M., Tao, H., Islam, A., et al. (2011). Epidermal electronics. Science *333*, 838–843. https://doi.org/10.1126/science.1206157.

3. Shin, J., Jeong, B., Kim, J., Nam, V.B., Yoon, Y., Jung, J., Hong, S., Lee, H., Eom, H., Yeo, J., et al. (2020). Sensitive wearable temperature

sensor with seamless monolithic integration. Adv. Mater. *32*, 1905527. https://doi.org/10.1002/adma.201905527.

4. Lee, J.W., Xu, R., Lee, S., Jang, K.-I., Yang, Y., Banks, A., Yu, K.J., Kim, J., Xu, S., Ma, S., et al. (2016). Soft, thin skin-mounted power management systems and their use in wireless thermography. Proc. Natl. Acad. Sci. USA *113*,

6131–6136. https://doi.org/10.1073/pnas.1605720113.

5. Webb, R.C., Bonifas, A.P., Behnaz, A., Zhang, Y., Yu, K.J., Cheng, H., Shi, M., Bian, Z., Liu, Z., Kim, Y.-S., et al. (2013). Ultrathin conformal devices for precise and continuous thermal characterization of human skin. Nat. Mater. *12*, 938–944. https://doi.org/10.1038/nmat3755.

6. Xu, B., Akhtar, A., Liu, Y., Chen, H., Yeo, W.-H., Park, S.I., Boyce, B., Kim, H., Yu, J., Lai, H.-Y., et al. (2016). An epidermal stimulation and sensing platform for sensorimotor prosthetic control, management of lower back exertion, and electrical muscle activation. Adv. Mater. *28*, 4462–4471. https://doi.org/10.1002/adma.201504155.

7. Yu, K.J., Kuzum, D., Hwang, S.-W., Kim, B.H., Juul, H., Kim, N.H., Won, S.M., Chiang, K., Trumpis, M., Richardson, A.G., et al. (2016). Bioresorbable silicon electronics for transient spatiotemporal mapping of electrical activity from the cerebral cortex. Nat. Mater. *15*, 782–791. https://doi.org/10.1038/nmat4624.

8. Fang, H., Yu, K.J., Gloschat, C., Yang, Z., Chiang, C.H., Zhao, J., Won, S.M., Xu, S., Trumpis, M., Zhong, Y., et al. (2017). Capacitively coupled arrays of multiplexed flexible silicon transistors for long-term cardiac electrophysiology. Nat. Biomed. Eng. *1*, 0038. https://doi.org/10.1038/s41551-017-0038.

9. Chiang, C.-H., Won, S.M., Orsborn, A.L., Yu, K.J., Trumpis, M., Bent, B., Wang, C., Xue, Y., Min, S., Woods, V., et al. (2020). Development of a neural interface for high-definition, long-term recording in rodents and nonhuman primates. Sci. Transl. Med. *12*, eaay4682. https://doi.org/10.1126/scitranslmed.aay4682.

10. Kim, T., Shin, Y., Kang, K., Kim, K., Kim, G., Byeon, Y., Kim, H., Gao, Y., Lee, J.R., Son, G., et al. (2022). Ultrathin crystalline-silicon-based strain gauges with deep learning algorithms for silent speech interfaces. Nat. Commun. *13*, 5815. https://doi.org/10.1038/s41467-022-33457-9.

11. Ferdous, N., and Ertekin, E. (2018). Atomic scale origins of sub-band gap optical absorption in gold-hyperdoped silicon. AIP Adv. *8*, 055014. https://doi.org/10.1063/1.5023110.

12. Starikov, S.V., Lopanitsyna, N., Smirnova, D.E., and Makarov, S.V. (2018). Atomistic simulation of Si-Au melt crystallization with novel interatomic potential. Comput. Mater. Sci. *142*, 303–311. https://doi.org/10.1016/j.commatsci.2017.09.054.

13. Bethala, B., and Premchand, K. (2005). Bulk silicon based temperature sensor. https://digitalcommons.usf.edu/etd/726.

14. Bracht, H., and Rodriguez Schachtrup, A. (1997). Diffusion of gold into heavily boron-doped silicon. MRS Proc. *469*, 25–36. https://doi.org/10.1557/PROC-469-25.

15. Brückner, B. (1971). Electrical properties of gold-doped silicon. Phys. Stat. Sol. *4*, 685–692. https://doi.org/10.1002/pssa.2210040312.

16. Bullis, W.M., and Strieter, F.J. (1968). Electrical properties of n-type silicon doped with gold. J. Appl. Phys. *39*, 314–318. https://doi.org/10.1063/1.1655751.

17. Mathiot, D. (1992). Gold, self-and dopant diffusion in silicon. Phys. Rev. B Condens. Matter *45*, 13345–13355. https://doi.org/10.1103/PhysRevB.45.13345.

18. Kanamori, S., and Sano, K. (1986). Low-distortion silicon thermistor with negative temperature coefficient of resistance. IEEE Trans. Comp. Hybrids Manufact. Technol. *9*, 317–320. https://doi.org/10.1109/TCHMT.1986.1136659.

19. Bullis, W.M. (1966). Properties of gold in silicon. Solid State Electron. *9*, 143–168. https://doi.org/10.1016/0038-1101(66)90085-2.

20. Collins, C.B., Carlson, R.O., and Gallagher, C.J. (1957). Properties of gold-doped silicon. Phys. Rev. *105*, 1168–1173. https://doi.org/10.1103/PhysRev.105.1168.

21. Mailoa, J.P., Akey, A.J., Simmons, C.B., Hutchinson, D., Mathews, J., Sullivan, J.T., Recht, D., Winkler, M.T., Williams, J.S., Warrender, J.M., et al. (2014). Room-temperature sub-band gap optoelectronic response of hyperdoped silicon. Nat. Commun. *5*, 3011. https://doi.org/10.1038/ncomms4011.

22. Brown, M., Jones, C.L., and Willoughby, A.F. (1975). Solubility of gold in p-type silicon. Solid State Electron. *18*, 763–770. https://doi.org/10.1016/0038-1101(75)90155-0.

23. Robert Thurber, W., Lewis, D.C., and Murray Bullis, W. (1973). Resistivity and Carrier Lifetime in Gold-Doped Silicon (Air Force Cambridge Research Laboratories, Air Force Systems Command, United States Air Force).

24. Hess, P. (1996). Laser diagnostics of mechanical and elastic properties of silicon and carbon films. Appl. Surf. Sci. *106*, 429–437. https://doi.org/10.1016/S0169-4332(96)00369-8.

25. Bhushan, B., and Li, X. (1997). Micromechanical and tribological characterization of doped single-crystal silicon and polysilicon films for microelectromechanical systems devices. J. Mater. Res. *12*, 54–63. https://doi.org/10.1557/JMR.1997.0010.

26. Gan, L., Ben-Nissan, B., and Ben-David, A. (1996). Modelling and finite element analysis of ultra-microhardness indentation of thin films. Thin Solid Films *290-291*, 362–366. https://doi.org/10.1016/S0040-6090(96)08972-9.

27. Rogers, J.A., Lagally, M.G., and Nuzzo, R.G. (2011). Synthesis, assembly and applications of semiconductor nanomembranes. Nature *477*, 45–53. https://doi.org/10.1038/nature10381.

28. Hopcroft, M.A., Nix, W.D., and Kenny, T.W. (2010). What is the Young's modulus of silicon? J. Microelectromech. Syst. *19*, 229–238. https://doi.org/10.1109/JMEMS.2009.2039697.

29. Kang, K., Cho, Y., and Yu, K.J. (2018). Novel nano-materials and nano-fabrication techniques for flexible electronic systems. Micromachines *9*, 263. https://doi.org/10.3390/mi9060263.

30. Zhang, Y., Yin, M., Baek, Y., Lee, K., Zangari, G., Cai, L., and Xu, B. (2020). Capillary transfer of soft films. Proc. Natl. Acad. Sci. USA *117*, 5210–5216. https://doi.org/10.1073/pnas.2000340117.

31. Okmi, A., Xiao, X., Zhang, Y., He, R., Olunloyo, O., Harris, S.B., Jabegu, T., Li, N., Maraba, D., Sherif, Y., et al. (2022). Discovery of graphene-water membrane structure: toward high-quality graphene process. Adv. Sci. *9*, 2201336. https://doi.org/10.1002/advs.202201336.